Applied Catalysis B: Environmental 174–175 (2015) 336–343

Contents lists available at ScienceDirect

Applied Catalysis B: Environmental

journal homepage: www.elsevier.com/locate/apcatb

Hierarchically structured ZSM-5 obtained by desilication as new catalyst for DME synthesis from methanol

M. Rutkowska*, D. Macina, N. Mirocha-Kubień, Z. Piwowarska, L. Chmielarz

Jagiellonian University, Ingardena 3, 30-060 Kraków, Poland

ARTICLE INFO

Article history:
Received 21 November 2014
Received in revised form 27 February 2015
Accepted 5 March 2015
Available online 7 March 2015

Keywords:
DME synthesis
ZSM-5
Desilication
Micro-mesoporous materials

ABSTRACT

A new type of micro–mesoporous materials with properties of ZSM-5 zeolite was tested as catalysts for the synthesis of dimethyl ether (DME) from methanol. The catalytic performance of ZSM-5 was improved by generation of mesoporosity using desilication method (alkaline leaching of framework Si). It was shown that controlled modification of the porous structure and acidity of the zeolitic samples strongly influences their catalytic activity, selectivity and stability in the process of DME synthesis. Desilication of ZSM-5 zeolite resulted in a development of the mesoporous structure and enhancement of its acidity, what was confirmed by N_2-sorption measurements, IR-DRIFT spectroscopy and NH_3-TPD. Desilicated zeolite samples exhibited higher catalytic activity and stability in the process of DME synthesis in comparison to parent ZSM-5. Moreover, micro–mesoporous zeolites were more resistant for poisoning by coke deposits in comparison to conventional ZSM-5 catalyst.

1. Introduction

One of the major problems of our times are the limited resources of fossil fuels. Moreover, emission of air pollutants (such as CO, NO_x, SO_x and soot) from mobile and stationary sources is one of the main reasons of environment degradation. These facts, together with a rapid depletion of petroleum reserves, are driving forces for development of new, alternative and clean fuels [1,2].

Dimethyl ether (DME, $H_3C—O—CH_3$) is one of the most promising clean alternative fuel and its large-scale production may partially stop extensive consumption of crude oil. DME can be used as an eco-friendly additive for diesel fuel due to its high cetane number (about 55–60), high oxygen content (34.8% by mass) and lack of C—C bond. Due to these properties the emission of CO, NO_x, SO_x and soot during its combustion is lower in comparison to common fossil fuels [1,2]. Moreover, DME has similar properties to propane and butane, the main components of LPG, and therefore, can be used as a LPG substitute [3].

Dimethyl ether can be produced by two methods: (i) direct (Eq. (1)), synthesis from syngas (STD, Syngas-to-DME) in a single reactor over a hybrid catalyst consisting of two functionalities – metallic for the synthesis of methanol from syngas and acidic for methanol dehydration to DME and (ii) indirect (Eq. (2)), dehydration of methanol over solid-acid catalysts (MTD, Methanol-to-DME) [1–5].

$$3CO + 3H_2 \leftrightarrow CH_3OCH_3 + CO_2 \quad (1)$$

$$2CH_3OH \leftrightarrow CH_3OCH_3 + H_2O \quad (2)$$

The indirect method (DME synthesis from alcohol over solid-acid catalysts) was reported first time by Mobil in 1965 [2,5]. The most common catalysts used for this process are solid acid materials such as γ-Al_2O_3 or ZSM-5 [1–7]. In general, it is suggested that the surface acidity of the catalyst is an essential parameter, which determines the spectrum of the reaction products formed during methanol dehydration. ZSM-5 exhibits higher catalytic activity than γ-Al_2O_3 because of its stronger acidity. On the other side, the catalysts containing strong acidic sites, such as zeolites, undergo faster deactivation due to deposition of coke and formation of other undesirable byproducts, what results in a decrease of selectivity to DME and limitation of the catalyst lifetime [4,7]. Above mentioned drawbacks of zeolites, limiting their catalytic application in the process of DME synthesis from methanol, could be overcome by generation of mesoporosity within the zeolite crystals and by adjustment of surface acidity.

The efficient approaches to create intracrystalline mesoporosity in zeolites and to control acidity are the silicon extraction by alkaline treatment and aluminum extraction by acidic treatment, respectively. Desilication in alkaline medium results in the formation of small amounts of mesopores or macropores, depending on the Si/Al ratio (high concentration of aluminum prevents the

* Corresponding author. Tel.: +48 126632096; fax: +48 126340515.
E-mail address: rutkowsm@chemia.uj.edu.pl (M. Rutkowska).

http://dx.doi.org/10.1016/j.apcatb.2015.03.006
0926-3373/

extraction of silicon from the zeolite framework). On the other side, dealumination, which occurs during steaming of zeolites or their treatment in acidic media, removes aluminum from the zeolite framework and therefore influences the acidic properties and enhances hydrothermal stability of zeolite [8–12]. Both desilication and dealumination of ZSM-5 zeolite are reported in the scientific literature. The group of Pérez-Ramírez widely studied the formation of mesopores in ZSM-5 zeolite by: (i) desilication in alkaline medium [13,14], (ii) sequential desilication-dealumination [15], (iii) desilication with organic hydroxides [16], (iv) desilication under microwave irradiation [17] and (v) desilication in alkaline medium in the presence of tetrapropylammonium or tetrabutylammonium hydroxide [18]. Moreover, Abelló et al. [16] compared the impact of tetraalkylammonium hydroxides and sodium hydroxide on the kinetics of mesopores formation in ZSM-5 zeolite. Groen et al. [19,20] proposed the mechanism of the mesoporosity formation in ZSM-5 zeolite by desilication in alkaline medium depending on the aluminum concentration in the zeolite framework. Despite the most frequently used desilication agent – NaOH [21], the scientists interest was also devoted to weaker alkaline solutions, such as, e.g., sodium [22–25] and calcium carbonates [25].

ZSM-5 with porosity enhanced by desilication was found to be a very efficient catalyst for steam reforming of DME (SRD) to syngas (H_2 + CO) [26–28]. The generation of mesopores in ZSM-5 resulted in a decreased rate of hydrocarbons and coke formation during SRD [26]. Thus, it seems possible that desilicated ZSM-5 will be also active, stable and selective catalysts for DME synthesis from methanol.

This paper presents the studies of catalytic performance of different types of porous materials (zeolites: Beta, Y and ZSM-5 and mesoporous silicas doped with aluminum: Al-SBA-15 and Al-MCF) in DME synthesis from methanol. Among the tested materials ZSM-5 was chosen for the further modifications (generation of mesoporosity by alkali treatment) in order to improve its activity and stability in DME synthesis. The influence of textural and surface properties of zeolites on their catalytic performance was analyzed.

2. Experimental methods

2.1. Catalysts preparation

Zeolite Beta (Si/Al∼21) was prepared via synthesis procedure described in our previous papers [29,30]. Zeolites Y (Si/Al∼16) and ZSM-5 (Si/Al∼16.5) were provided by Eka Chemicals.

Mesoporous silicas (SBA-15 and MCF) were used as supports for alumina species deposition. SBA-15 was synthesized according to the slightly modified procedure described earlier by Chmielarz et al. [31]. The synthesis method of MCF was given previously by Meynen et al. [32]. In the next step, the surface of mesoporous silicas was modified by anchoring of organic molecules to generate the ion-exchange properties according to the modified procedure described earlier by Trejda et al. [33]. Both SBA-15 and MCF, were thermally treated at 200 °C for 2 h in order to remove adsorbed water. In a next step, 2 g of mesoporous silica was dispersed in 50 mL of toluene (POCH) (previously dried with ZSM-5 zeolite). The obtained mixture was heated to 100 °C and stirred for 30 min. Subsequently, 1.85 mL of 3-(mercaptopropyl) trimethoxysilane (MPTMS, Sigma–Aldrich) was added dropwise and the obtained mixture was stirred at the same temperature for next 20 h. After filtration, modified silica material was washed with toluene (150 mL) and distillated water (800 mL). Finally, the samples were dried at 60 °C for 8 h. In the next step, mesoporous silicas modified with MPTMS were treated with a solution of H_2O_2 (POCH) in order to convert —SH groups to—SO_3H. In each case, 2 g of modified material was dispersed in 30% aqueous solution of H_2O_2 (40 mL). Then the obtained slurry was stirred at room temperature (RT) for 24 h. Subsequently, the sample was separated by filtration, washed with distillated water and ethanol and finally dried at 60 °C for 8 h.

The modified silicas (with—SO_3H groups) were modified with aluminum oligocations (according to procedure described in [34]). An appropriate volume of 0.1 M aqueous solution of NaOH was slowly added into $AlCl_3$ solution under constant stirring until the molar ratio of OH^-/Al^{3+} reached 2.4. In the next step, the obtained solution was aged at RT for two weeks. After this time, a calculated amount of the pillaring solution was added dropwise into the suspension containing 1 wt.% of modified silicas dispersed in distillated water until the Al^{3+}/modified silica ratio reached the value of 1 mmol Al^{3+}/g of modified silica. The obtained suspensions mixtures were vigorously stirred at RT for 24 h. After that time, the obtained solid products were separated by filtration, washed with distillated water until complete removal of chloride anions and dried at 120 °C for 12 h. Finally, the samples were calcined at 500 °C for 12 h with a heating rate of 1 °C/min. The obtained samples were denoted as Al-SBA-15 and Al-MCF.

The alkaline treatment of ZSM-5 was performed using a volume of 75 mL of 0.1 M NaOH solution (Chempur) per 1 g of zeolite. The resulting slurry was stirred under reflux at 80 °C for 1, 2 and 4 h. After filtration zeolites were washed with distilled water (3 times with 25 mL) and dried in ambient conditions. In the next step, the obtained samples (ZSM-5/1h, ZSM-5/2h and ZSM-5/4h) were calcined in air atmosphere at 600 °C for 6 h.

The Na-forms of the obtained samples were triple exchanged with a solution of NH_4NO_3 (0.5 M, Sigma–Aldrich) at 80 °C for 1 h, filtered, washed (3 times with 25 mL of double distilled H_2O) and dried in ambient conditions. Finally, the samples were calcined at 600 °C for 6 h to convert them to H-forms.

2.2. Catalysts characterization

The textural parameters of the samples were determined by N_2 sorption at −196 °C using a 3Flex v1.00 (Micromeritics) automated gas adsorption system. Prior to the analysis, the samples were degassed under vacuum at 350 °C for 24 h. The specific surface area (S_{BET}) of the samples was determined using BET (Brunauer–Emmett–Teller) model according to Rouquerol recommendations [35]. The micropore volume (at p/p_0 = 0.98) and specific surface area of micropores were calculated using the Harkins and Jura model (*t*-plot analysis). Mesopore volume was calculated from desorption branch using BJH model (Kruk–Jaroniec–Sayari empirical procedure) in the range of 17-300 Å.

The X-ray diffraction (XRD) patterns of the samples were recorded using a Bruker D2 Phaser diffractometer. The measurements were performed in the 2 theta range of 5–50° with a step of 0.02°.

IR measurements were performed using a Nicolet 6700 FT-IR spectrometer (Thermo Scientific) equipped with DRIFT (diffuse reflectance infrared Fourier transform) accessory and DTGS detector. The dried samples were grounded with dried potassium bromide powder (4 wt.%). The measurements were carried out in the wavenumber range of 400–4000 cm^{-1} with a resolution of 2 cm^{-1}.

Surface acidity (concentration and strength of acid sites) of the samples was studied by temperature-programmed desorption of ammonia (NH_3-TPD). The measurements were performed in a flow microreactor system equipped with QMS detector (VG Quartz). Prior to ammonia sorption, a sample was outgassed in a flow of pure helium at 688 K for 30 min. Subsequently, microreactor was cooled to 343 K and the sample was saturated in a flow of gas mixture containing 1 vol.% of NH_3 in helium for about 120 min. Then, the catalyst was purged in a helium flow until a constant base line level

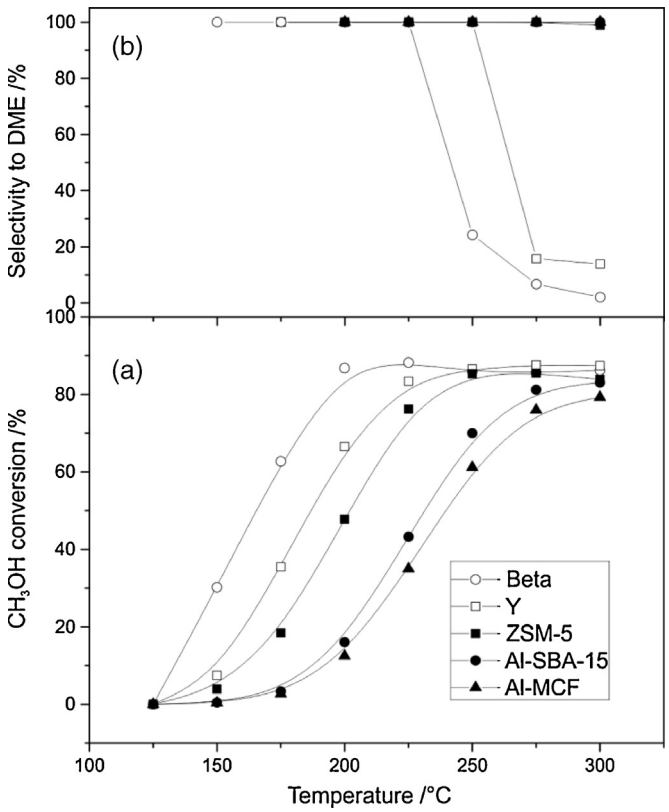

Fig. 1. Temperature dependence of CH_3OH conversion (a) and selectivity (b) to DME over different types of catalysts. Conditions: 4 vol. % CH_3OH; He as balancing gas; total flow rate – 20 mL/min; weight of catalyst – 0.1 g.

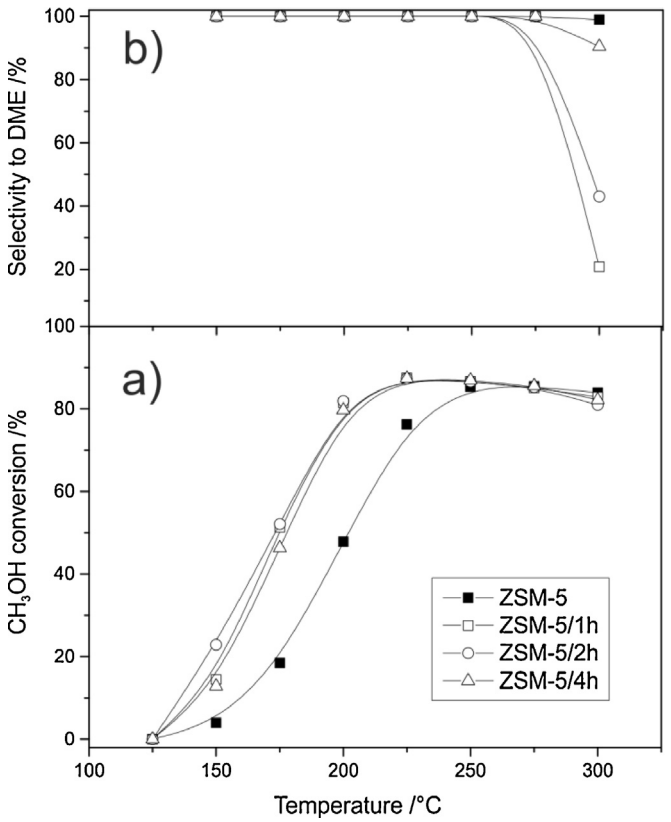

Fig. 2. Temperature dependence of CH_3OH conversion (a) and selectivity (b) to DME over ZSM-5 and desilicated zeolites. Conditions: 4 vol. % CH_3OH; He as balancing gas; total flow rate – 20 mL/min; weight of catalyst – 0.1 g.

was attained. Desorption was carried out with a linear heating rate (10 °C/min) in a flow of He (20 mL/min). Calibration of QMS with commercial mixtures allowed recalculating detector signal into the rate of NH_3 evolution.

Thermogravimetric measurements were performed using a TGA/SDTA851^e Mettler Toledo instrument connected with quadrupole mass spectrometer ThermoStar (Balzers). The samples were heated in a flow of synthetic air (80 mL/min) with the ramping of 10 °C/min, in the temperature range of 70–600 °C.

2.3. Catalytic tests

Catalytic experiments for the process of DME synthesis from methanol were performed in a fixed-bed quartz microreactor system under atmospheric pressure in the temperature range from 125 to 300 °C in intervals of 25 °C. For each test, 0.1 g of catalyst with a particle size between 0.160 and 0.315 mm was outgassed in a flow of pure helium at 300 °C for 1 h. After cooling down to 125 °C, the gas mixture containing 4 vol.% of methanol diluted in pure helium (total flow rate of 20 mL/min) was supplied into the reactor using isothermal saturator (0 °C). To avoid any product condensation during the reaction run, the gas lines were heated to 120 °C using heating tapes. The outlet gases were analyzed using a gas chromatograph (SRI 8610C) equipped with methanizer and FID detector. Additionally, the catalytic stability (24 h of continues work) at different temperatures was investigated for the ZSM-5 and ZSM-5/1h samples.

3. Results and discussion

Results of the catalytic studies of different types of materials (Beta, Y and ZSM-5 zeolites and mesoporous materials: Al-SBA-15 and Al-MCF) in the process of DME synthesis from methanol are presented in Fig. 1. The highest methanol conversion (Fig. 1a) was observed for the process performed in the presence of zeolite Beta. The following order of the samples activity was found: Beta > Y > ZSM-5 > Al-SBA-15 > Al-MCF. On the other side, selectivity to DME (Fig. 1b) strongly decreased in case of the most active

Table 1
Samples acidity measured by NH_3-TPD.

Sample code	Total concentration of acid sites /μmol/g	Concentration of low temp. acid sites /μmol/g	Concentration of high temp. acid sites /μmol/g	Surface density of acid sites /μmol/m^2
Beta	529	---	---	0.809
Y	482	---	---	0.583
Al-SBA-15	229	---	---	0.475
Al-MCF	147	---	---	0.304
ZSM-5	209	89	146	0.537
ZSM-5/1h	256	86	144	0.642
ZSM-5/2h	297	88	361	0.615
ZSM-5/4h	316	134	241	0.591

samples (zeolites Beta and Y) at temperatures above 250 °C, while for the other samples reminded close to 100% in the whole studied temperature range (up to 300 °C). Acid sites are the most likely considered as active centers of the synthesis of DME. Thus, in order to prove this hypothesis and obtain more information about surface concentration and strength of acid sites in the samples the NH_3-TPD measurements were done (Table 1). As it can be seen, the conversion of methanol increases together with the increase in the surface density of acid sites, what proves the statement, that the efficiency of DME synthesis strongly depends on acidity of the catalyst. However, it must be noted that for the most active samples (Beta and Y) selectivity to DME rapidly droops at higher temperatures. This phenomenon can be related to the presence of micropores (Table 2), which together with very high surface density of acid sites favors the formation of byproducts. On the other hand, high selectivity to DME, obtained over the aluminum modified mesoporous silicas, could be explained by the presence of mesopores in their structure, what resulted in an improved diffusion of the reactants through the catalyst grains and therefore, the formation of byproducts was limited.

The obtained results showed that acidity of ZSM-5 zeolite, among tested catalysts, seems to be optimal to obtain relatively high catalytic activity with satisfactory selectivity to DME in a wide temperature region. Thus, in a second part of the research, ZSM-5 was selected for more detailed studies including its desilication to improve catalytic performance in the synthesis of DME.

The results of the catalytic studies of parent ZSM-5 and its desilicated modifications (ZSM-5/1h, ZSM-5/2h, ZSM-5/4h) in the process of DME synthesis from methanol are presented in Fig. 2. The alkaline treatment of ZSM-5 resulted in an increase of the methanol conversion to DME (Fig. 2a). The observed enhanced catalytic activity can be connected with the mesoporosity generated during desilication process (Table 2). The alkaline treated samples exhibit a very similar activity in DME synthesis, thus, it was concluded that duration of alkali treatment did not affect significantly activity of the zeolite based catalysts. The DME selectivity (Fig. 2b) at temperatures above 275 °C clearly depends on duration of desilication process and significantly increases with the increasing of alkali treatment duration. This effect can be related to increased acidity of desilicated zeolites (Table 1) (favorable byproducts formation), which on the other side was balanced by generated mesoporosity (the best selectivity to DME was obtained for ZSM-5/4h). However, it should be also noted that the highest selectivity to DME was obtained for ZSM-5 non-modified with NaOH.

Table 2
Textural properties of the samples determined from the N_2-sorption measurements.

Sample code	S_{BET} /m^2/g	S_{MIC} /m^2/g	S_{EXT} /m^2/g	V_{MIC} /cm^3/g	V_{MES} /cm^3/g
Beta	654	598	55	0.239	0.141
Y	826	765	62	0.311	0.239
Al-SBA-15	482	116	366	0.044	0.630
Al-MCF	484	44	440	0.011	1.420
ZSM-5	389	356	33	0.157	0.090
ZSM-5/1h	399	364	35	0.158	0.098
ZSM-5/2h	483	361	121	0.160	0.186
ZSM-5/4h	535	226	309	0.087	0.380

Textural parameters of the parent ZSM-5 sample and desilicated ZSM-5/1h, ZSM-5/2h and ZSM-5/4h, determined by nitrogen sorption measurements, are presented in Table 2. Textural properties of ZSM-5 and ZSM-5/1h are very similar and only slight increase in mesoporosity was observed for the desilicated sample. These results suggest that the applied conditions of alkali treatment (1 h, 80 °C, 0.1 M NaOH) were too mild to significantly develop mesoporosity in ZSM-5. The extension of the alkali treatment duration

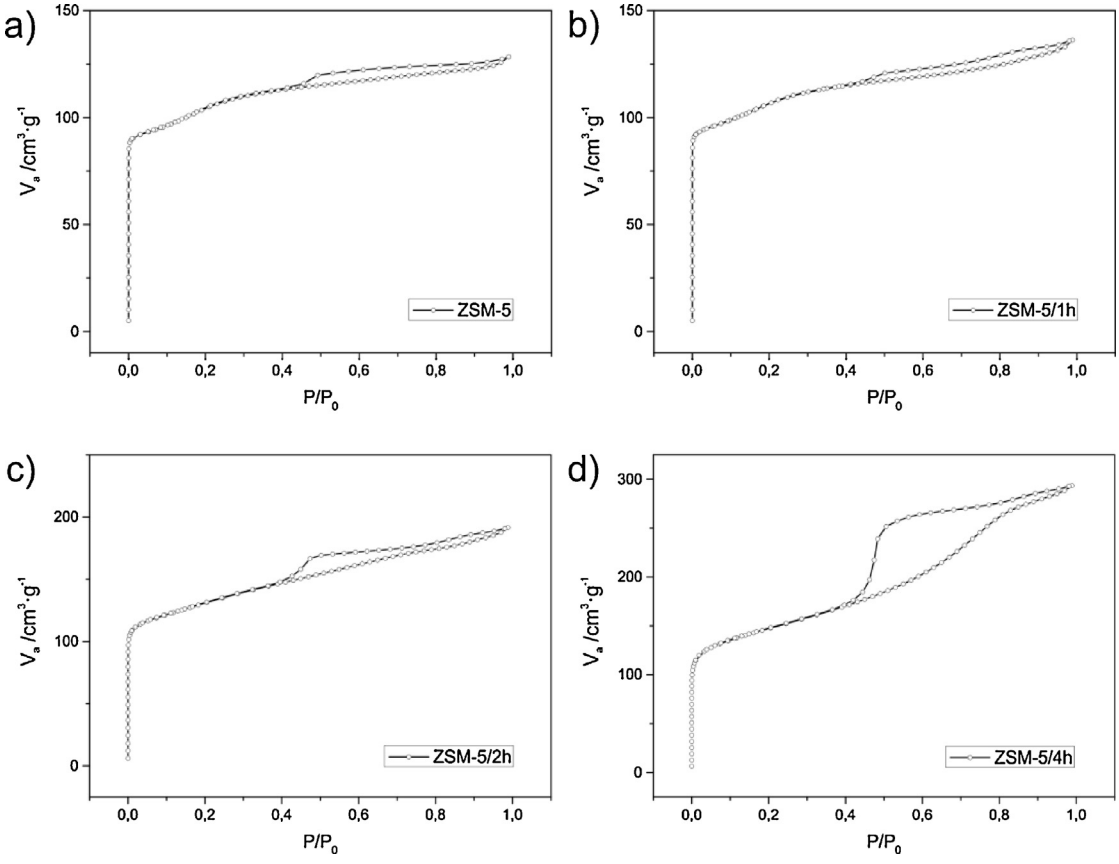

Fig. 3. Nitrogen adsorption–desorption isotherms of ZSM-5 (a) and its desilicated forms (b–d).

to 2 h resulted in a more effective development of mesoporosity in zeolite. In this case, the sample (ZSM-5/2h) was characterized by a significantly higher BET surface area, external surface area and volume of mesopores in comparison to parent ZSM-5. It is worth to notice that development of mesoporosity in ZSM-5/2h proceeded with the maintenance of microporosity in ZSM-5 zeolite. While, in case of the sample, alkali treated for 4 h (ZSM-5/4h) generation of mesoporosity (mesopore volume about 4 times higher in comparison to parent ZSM-5) was connected with a partial destruction of the microporous zeolite structure. The analysis of textural parameters of the desilicated samples leads to the conclusion that the alkaline treatment of ZSM-5 for two hours was the most efficient to develop mesoporosity with simultaneous preserving of microporosity.

The nitrogen adsorption–desorption isotherms, recorded for the parent ZSM-5 sample and desilicated ZSM-5/1h, ZSM-5/2h and ZSM-5/4h, are shown in Fig. 3a–d, respectively. The isotherm of type I [36] (according to the IUPAC classification), characteristic of the microporous structure, was recorded for parent ZSM-5. While, in case of the desilicated samples, the adsorption–desorption isotherms form hysteresis loops: (i) of type H4, characteristic for micro–mesoporous materials with narrow slit-shaped like pores, in case of ZSM-5/1h and ZSM-5/2h and (ii) a hybrid of H4 and H2 hysteresis (characteristic for pores with not well defined shape and size) types in case of ZSM-5/4h [36]. The hysteresis loops obtained in case of the desilicated samples proved the successful generation of mesopores, especiallyin case of ZSM-5/4h.

The XRD powder patterns of the parent ZSM-5 sample and its desilicated forms – ZSM-5/1h, ZSM-5/2h and ZSM-5/4h are shown in Fig. 4. Reflections characteristic of the MFI topology [37] are present in all diffractograms, what proves the zeolitic character of the samples and the maintenance of this character after desilication process. The intensity of the XRD reflections decreased with an extension of alkaline treatment duration. The ZSM-5/4h sample is significantly less crystalline than parent ZSM-5, what can be related to partial destruction of the zeolite structure during desilication process (what is in agreement with the nitrogen sorption results).

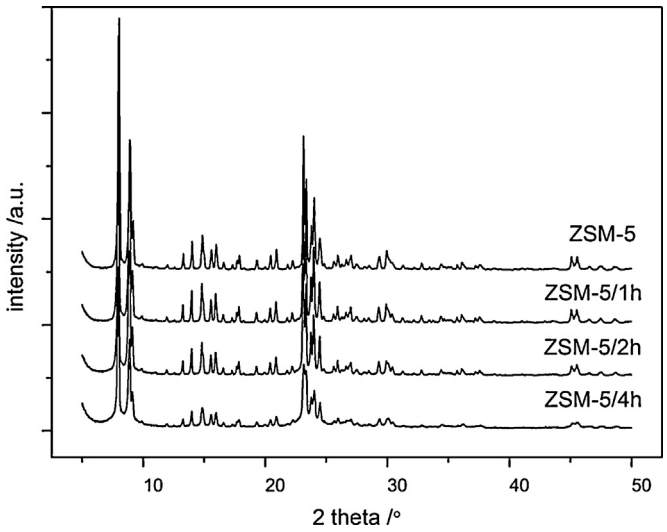

Fig. 4. XRD patterns of ZSM-5 and its desilicated forms.

DRIFT spectra, recorded for parent ZSM-5 and its desilicated forms – ZSM-5/1h, ZSM-5/2h and ZSM-5/4h, are shown in Fig. 5. A broad band at about 2500–3700 cm^{-1} and intense peak at about 900–1300 cm^{-1} (Fig. 5a), present in all the spectra, are assigned to OH stretching of defective Si—OH and framework asymmetric vibrations in silica materials, respectively [38]. After desilication of zeolite, the significant changes in the OH region (about 3000–3800 cm^{-1}) were found (Fig. 5b). An increase in intensity of the band around 3745 cm^{-1} (observed mainly in case of ZSM-5/4h), connected with vibrations of terminal silanol groups, indicates a development of the external surface of the zeolite crystals and mesopore surface [39,40]. The bands at about 3610 cm^{-1}

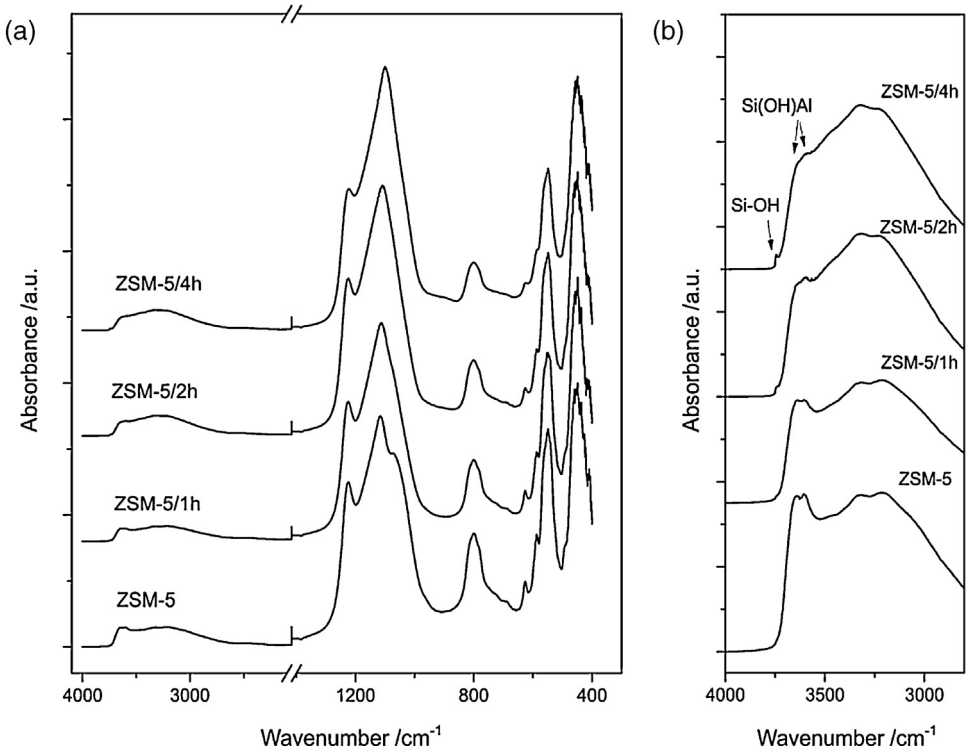

Fig. 5. DRIFT spectra of ZSM-5 and its desilicated forms.

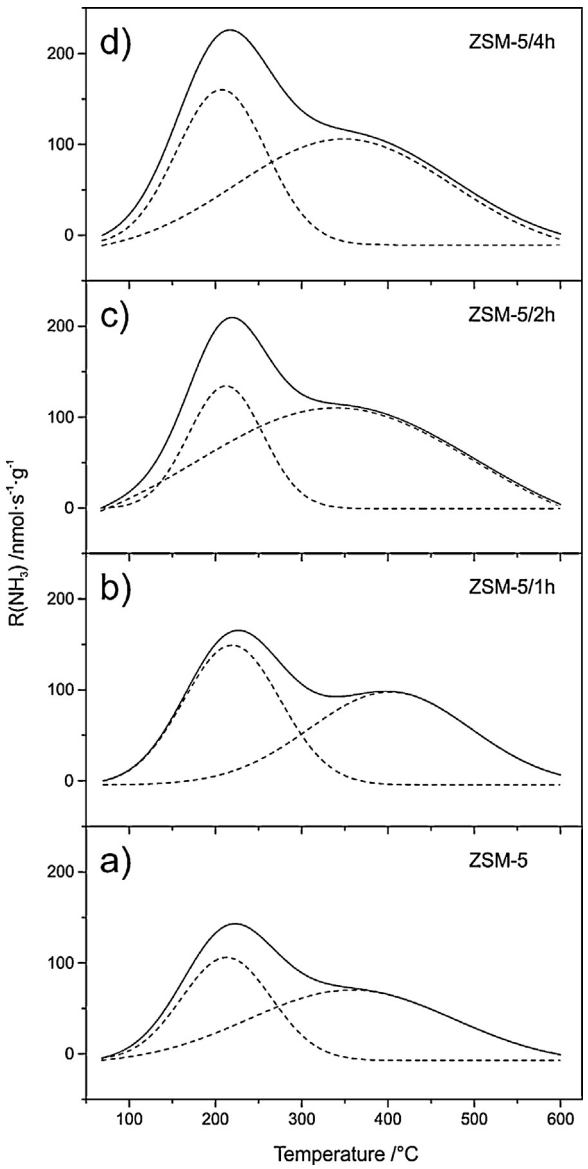

Fig. 6. NH_3-TPD profiles of ZSM-5 (a) and its desilicated forms (b–d). Conditions: 1 vol. % NH_3 in He; gas flow 20 mL/min; weight of catalyst – 0.05 g.

resulting from Si—(OH)—Al vibrations in the zeolite framework (Brønsted acidity) decreased after desilication process. This observation suggests removal of both Si and Al from the zeolite framework [12]. The generation of mesoporosity by silicon extraction changes the framework Al environment and therefore, causes the remarkable behavior of aluminum, such as re-alumination [13,40].

Acidic properties of parent ZSM-5 and the alkali-treated samples were studied using NH_3-TPD method (Fig. 6). In all TPD profiles, two peaks representing ammonia bounded to weaker (maximum at about 225 °C) and stronger acid sites (maximum at about 400 °C) were found. According to literature reports [19,41], the low-temperature peak could be attributed to weak Lewis type acid sites (e.g., extra-framework aluminum), while the high-temperature peak to ammonia interacting with framework Al (Brønsted acid sites). The shape of ammonia desorption profiles was only slightly modified for desilicated samples. The main difference is related to the increased intensity of ammonia desorption profiles recorded for the alkaline treated samples. Moreover, it can be noted that the peak at about 400 °C is reduced in favor of the peak at about

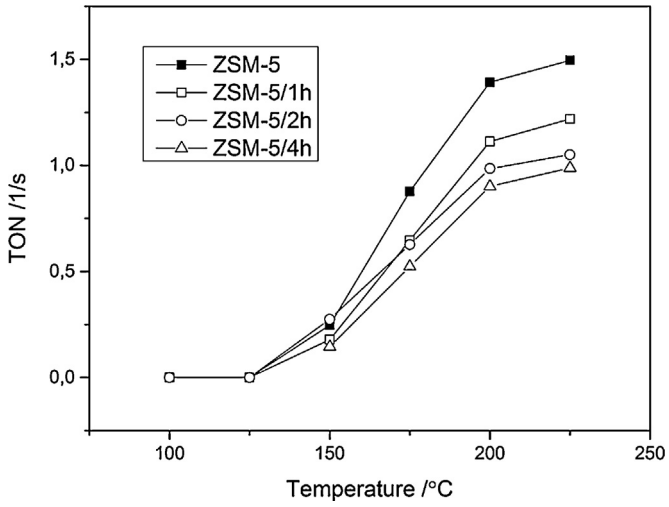

Fig. 7. Temperature dependence of TON for ZSM-5 and its desilicated forms.

225 °C in case of ZSM-5/2h and ZSM-5/4h (Fig. 6c and d). A decrease in Brønsted acidity after desilication (especially, for zeolite alkali treated for 2 or 4 h) are in agreement with the results of IR-DRIFT studies.

Surface concentration and density of acid sites determined for ZSM-5 and its modifications are presented in Table 1. The concentration of acid sites was calculated by integration of areas under TPD profiles, which were recalculated into a number of adsorbed ammonia molecules. It was assumed that one NH_3 molecule adsorb on one acid site. The value of total concentration of acid sites increased after alkali treatment of ZSM-5 and was dependent on duration of this process. This effect could be explained by partial extraction of Si atoms, what increased the relative Al content in the samples [8,42]. The concentration of strong sites (high-temperature peak) significantly changed after 2 h of alkali treatment, what was probably connected with enhanced accessibility of framework Al. While the concentration of weak acid sites (low-temperature peak) increased after 4 h of desilication, what can be related to the enhanced Lewis acidity, caused by the Al extra framework deposits [9]. However, it should be taken into account that this type of analysis (basing on deconvoluted TPD profiles) gives only approximate information about the content of particular types of acid sites.

In order to investigate the efficiency of acid sites in parent ZSM-5 and in the alkali-treated samples in the synthesis of DME, we calculated the turn over number (TON) assuming that each acid site plays a role of active site (in calculations, the concentration of acid sites determined from NH_3 sorption measurements was used) (Fig. 7). The most active acid centers are present in conventional ZSM-5. The catalytic efficiency of acid sites decreased together with an increase in duration of alkali treatment [43–46]. Thus, we can suppose that the catalytic activity of acid sites diminished after desilication (disturbed crystalline structure). On the other side, alkali treatment of zeolite resulted in a significant increase of the surface concentration of acid sites, what finally resulted in a higher catalytic activity of the micro–mesoporous samples in comparison to convectional ZSM-5. Concluding, it could be suggested that the mesoporous zeolites are characterized by a higher concentration of the less catalytically active acid sites.

Fig. 8 shows the results of stability tests for two selected catalysts – parent ZSM-5 (reaction at 225, 250 and 275 °C) and ZSM-5/1h (reaction at 200, 225 and 250 °C) performed for 24 h (temperatures of the catalytic tests were selected to analyze the catalysts stability for methanol conversion of about 80–90%). The methanol conversion in the presence of parent ZSM-5 at 225 and 250 °C decreased by about 2–3%, while in case of desilicated zeolite (ZSM-5/1h),

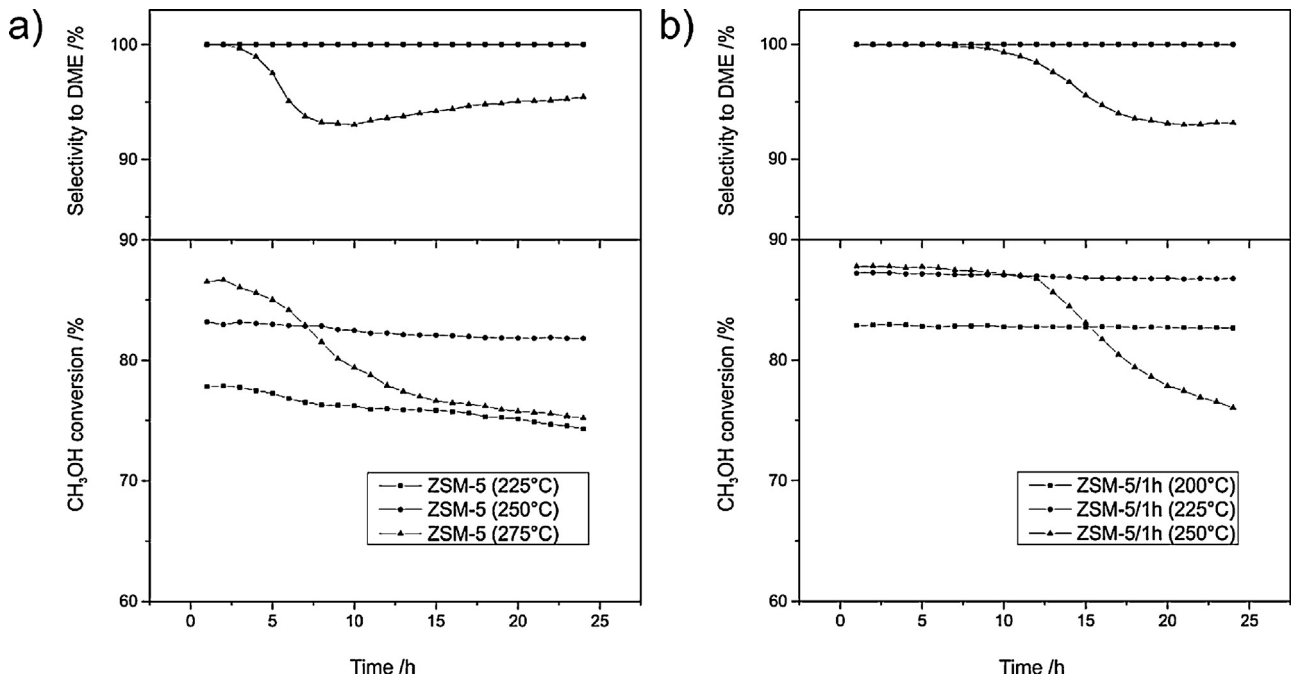

Fig. 8. Time dependence (stability tests: 24 h at different temp.) of CH_3OH conversion and selectivity to DME of: ZSM-5 (a) and ZSM-5/1 h (b). Conditions: 4 vol. % CH_3OH; He as balancing gas; total flow rate – 20 mL/min; weight of catalyst – 0.1 g.

any changes in the methanol conversion at 200 and 225 °C were observed. In case of both the samples, DME was the only reaction product at these temperatures. Much more significant changes were observed at 275 °C for ZSM-5 and at 250 °C for ZSM-5/1h. Deactivation of the ZSM-5 sample started after 2 h of test and after 24 h, the methanol conversion decreased by about 11%, while for the ZSM-5/1h, a decrease in the efficiency of the DME synthesis started after 12 h of the catalytic test. In case of both the samples, the changes in methanol conversion were accompanied by a decrease in selectivity to DME. These effects are related to the formation of coke deposits in the pore system of the zeolite samples, what was evidenced also by the color change of the ZSM-5 (275 °C) and ZSM-5/1h (250 °C) samples [1,47].

The content and nature of the carbon deposits formed in the samples during stability tests were studied using thermogravimetric analysis coupled with QMS detection of gas products. The experiments were performed in a flow of synthetic air. The m/e signal of 44 (QMS) was analyzed to detect the evolution of CO_2 – gas product of coke deposit oxidation. For the ZSM-5/1h sample after stability tests performed at 200 and 225 °C evolution of CO_2 was not detected. While, in case of the ZSM-5 (225 °C) and ZSM-5 (250 °C) samples, a small peak of CO_2 evolution in the temperature range of 370–470 °C, related to combustion of carbon deposit, was detected (results not shown). The evolution of CO_2 at relatively low temperature as well as evolution in the same temperature range of water vapor ($m/e = 18$) suggest that the formed coke deposit apart from carbon contains also hydrogen. It is known that the formation of coke deposits during the DME synthesis is a result of the side-reactions. DME is firstly converted to light olefins (mainly to ethylene and propylene) and at higher temperatures mainly to paraffins and alkyl aromatics [48,49]. It is very important to mention that the content of coke deposit formed in these samples during 24 h of stability test, estimated from the TG-QMS studies, is only about 400 ppm.

For the ZSM-5 (275 °C) and ZSM-5/1h (250 °C) samples, the evolution of higher amount of CO_2 was detected. Fig. 9 presents the CO_2 evolution profiles of these two catalysts after 24 h of stability test. In case of both the samples the weight loss was similar and equal to

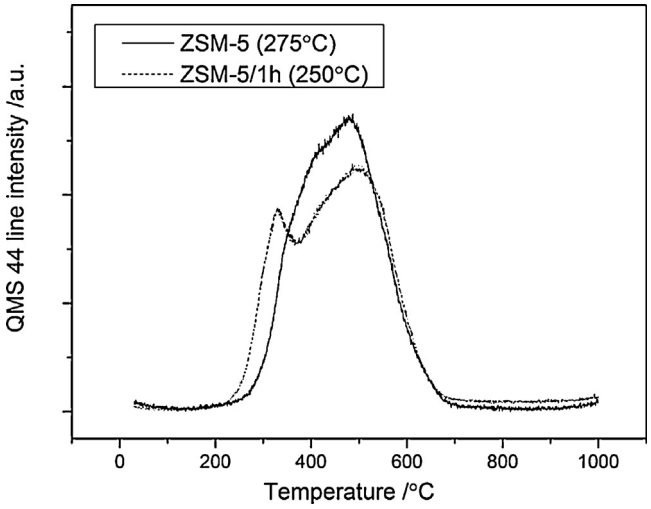

Fig. 9. CO_2 evolution signals measured by QMS for the samples ZSM-5 (275 °C) and ZSM-5/1h (250 °C) after 24 h of stability test.

about 6%, however, two peaks of CO_2 evolution were identified in the profile recorded for the mesoporous sample. These peaks can be related to different nature of formed coke. The first peak at about 330 °C can be attributed to the slightly developed coke, while the second one (at about 500 °C) to the more condensed forms of coke deposit (with a lower H/C ratio). The presence of two well-defined peaks in case of the ZSM-5/1h sample can be explained by the coke combustion in meso and macropores (low-temperature peak) and in the zeolite micropores (high-temperature peak) [50].

4. Conclusions

In the undertaken research, the activity and stability of a new group of micro–mesoporous materials in the process of dimethyl ether synthesis from methanol was studied.

In a first step different materials (zeolites: Beta, Y and ZSM-5 and mesoporous silicas doped with alumina: Al-SBA-15 and Al-MCF) were compared with respect to their porous structure and acidity. It seems that acidity of the catalysts is a crucial parameter in DME synthesis – too high surface density of acid sites and additionally the presence of micropores is responsible for the formation of byproducts and poisoning of the catalyst by coke deposition. Among the analyzed catalysts, taking into account high catalytic activity and selectivity to DME in a wide temperature region, ZSM-5 zeolite was found to be the most promising for this reaction.

In a second part of the research, the porosity and acidity of parent ZSM-5 was modified by desilication (silicon extraction in alkaline medium) to enhance its activity in DME synthesis. Alkaline treatment resulted in a significant development of BET surface area and volume of mesopores. Moreover, by the change in relative Si/Al ratio, the concentration of acid sites in the desilicated samples increased, however, as it was stated from TON calculations, the catalytic efficiency of acid sites in the micro–mesoporous samples is lower in comparison to non-modified ZSM-5.

The samples modified by controlled alkaline leaching were found to be more active in comparison to parent ZSM-5, what can be connected with a higher total concentration of acid sites in these samples. Moreover, our studies have shown that micro–mesoporous zeolites were more resistant for poisoning by coke deposits in comparison to classical ZSM-5 zeolite. It could be explained by modification of acid sites during alkali treatment, which were less active in coke formation. Another important issue is more "open" porous structure in case of the alkali treated samples and therefore, the risk of pore plugging by coke deposit is lower.

Acknowledgements

This work was supported by the National Science Center under grant no. 2011/03/N/ST5/04820. L.C., D.M. and Z.P. acknowledge the financial support from the grant no. 2012/05/B/ST5/00269 from the Polish Ministry of Science. Part of the research was carried out with the equipment purchased thanks to the financial support of the European Regional Development Fund in the framework of the Polish Innovation Economy Operational Program (contract no. POIG.02.01.00-12-023/08).

References

[1] Q. Yang, M. Kong, Z. Fan, X. Meng, J. Fei, F.-S. Xiao, Energy Fuels 26 (7) (2012) 4475–4480.
[2] A.I. Osman, J.K. Abu-Dahrieh, D.W. Rooney, S.A. Halawy, M.A. Mohamed, A. Abdelkader, Appl. Catal. B: Environ. 127 (2012) 307–315.
[3] K.C. Tokay, T. Dogu, G. Dogu, Chem. Eng. J. 184 (2012) 278–285.
[4] J. Abu-Dahrieh, D. Rooney, A. Goguet, Y. Saih, Chem. Eng. J. 203 (2012) 201–211.
[5] Q. Tang, H. Xu, Y. Zheng, J. Wang, H. Li, J. Zhang, Appl. Catal. A: Gen. 413–414 (2012) 36–42.
[6] M. Xu, J.H. Lunsford, D.W. Goodman, A. Bhattacharyya, Appl. Catal. A: Gen. 149 (2) (1997) 289–301.
[7] V.V. Volkov, E.G. Novitskii, G.A. Diøov, P.V. Samokhin, M.A. Kipnis, A.B. Yaroslavtsev, Catal. Today 193 (2012) 31–36.
[8] M.S. Holm, K. Egeblad, P.N.R. Vennestrøm, C.G. Hartmann, M. Kustova, C.H. Christensen, Eur. J. Inorg. Chem. 33 (2008) 5185–5189.
[9] D. Verboekend, S. Mitchell, M. Milina, J.C. Groen, J. Pérez-Ramírez, J. Phys. Chem. 115 (2011) 14193–14203.
[10] J.C. Groen, G.M. Hamminga, J.A. Moulijn, J. Pérez-Ramírez, Phys. Chem. Chem. Phys. 9 (2007) 4822–4830.
[11] F.C. Meunier, D. Verboekend, J.-P. Gilson, J.C. Groen, J. Pérez-Ramírez, Micropor. Mesopor. Mater. 148 (2012) 115–121.
[12] B. Gil, Ł. Mokrzycki, B. Sulikowski, Z. Olejniczak, S. Walas, Catal. Today 152 (2010) 24–32.
[13] J.C. Groen, L.A.A. Peffer, J.A. Moulijn, J. Pérez-Ramírez, Colloids Surf. A 241 (2004) 53–58.
[14] J.C. Groen, T. Bach, U. Ziese, A.M. Paulaime-Van Donk, J. Pérez-Ramírez, J. Am. Chem. Soc. 127 (2005) 10792–10793.
[15] J.C. Groen, J.A. Moulijn, J. Pérez-Ramírez, Micropor. Mesopor. Mater. 87 (2005) 153–161.
[16] S. Abelló, A. Bonilla, J. Pérez-Ramírez, Appl. Catal. A:Gen. 364 (2009) 191–198.
[17] S. Abelló, J. Pérez-Ramírez, Phys. Chem. Chem. Phys. 11 (2009) 2959–2963.
[18] J. Pérez-Ramírez, D. Verboekend, A. Bonilla, S. Abelló, Adv. Funct. Mater. 19 (2009) 3972–3979.
[19] J.C. Groen, L.A.A. Peffer, J.A. Moulijn, J. Pérez-Ramírez, Chem. Eur. J. 11 (2005) 4983–4994.
[20] J.C. Groen, J.A. Moulijn, J. Pérez-Ramírez, J. Mater. Chem. 16 (2006) 2121–2131.
[21] M. Ogura, S.-Y. Shinomiya, J. Tateno, Y. Nara, M. Nomura, E. Kikuchi, M. Matsukata, Appl. Catal. A: Gen. 219 (2001) 33–43.
[22] R. Le Van Mao, S. Xiao, A. Ramsaran, J. Yao, J. Mater. Chem. 4 (1994) 605–610.
[23] R. Le Van Mao, A. Ramsaran, S. Xiao, J. Yaot, V. Semme, J. Mater. Chem. 5 (1995) 533–535.
[24] D. Ohayon, R. Le Van Mao, D. Ciaravino, H. Hazel, A. Cochennec, N. Rolland, Appl. Catal. A: Gen. 217 (2001) 241–251.
[25] S. Fathi, M. Sohrabi, C. Falamaki, Fuel 116 (2014) 529–537.
[26] A.G. Gayubo, J. Vicente, J. Ereña, L. Oar-Arteta, M.J. Azkoiti, M. Olazar, J. Bilbao, Appl. Catal. A: Gen 483 (2014) 76–84.
[27] J. Ereña, J. Vicente, A.T. Aguayo, A.G. Gayubo, M. Olazar, J. Bilbao, Int J. Hydrogen Energy 38 (2013) 10019–10028.
[28] J. Vicente, A.G. Gayubo, J. Ereña, A.T. Aguayo, M. Olazar, J. Bilbao, Appl. Catal. B: Environ. 130–131 (2013) 73–83.
[29] M. Rutkowska, L. Chmielarz, D. Macina, Z. Piwowarska, B. Dudek, A. Adamski, S. Witkowski, Z. Sojka, L. Obalová, C. Van Oers, P. Cool, Appl. Catal. B: Environ. 146 (2014) 112–122.
[30] M. Rutkowska, Z. Piwowarska, E. Micek, L. Chmielarz, Micropor. Mesopor. Mat. http://dx.doi.org/10.1016/j.micromeso.2014.10.011
[31] L. Chmielarz, P. Kuśtrowski, R. Dziembaj, P. Cool, E.F. Vansant, Micropor. Mesopor. Mater. 127 (2010) 133–141.
[32] V. Meynen, P. Cool, E.F. Vansant, Micropor. Mesopor. Mater. 125 (2009) 170–223.
[33] M. Trejda, K. Stawicka, A. Dubinska, M. Ziolek, Catal. Today 187 (2012) 129–134.
[34] D. Macina, P. Drużkowski, R. Dębek, M. Rutkowska, A. Kowalczyk, A. Węgrzyn, M. Motak, T. Grzybek, L. Chmielarz, 6th Int. Ann. Meet. GDRI Catal. Proc. (2013) 184–191.
[35] J. Rouquerol, P. Llewellyn, F. Rouquerol, Stud. Surf. Sci. Catal. 160 (2007) 49.
[36] S. Lowell, E. Joan Shields, A. Martin Thomas, M. Thommes, Part. Technol. Ser. 16 (2004).
[37] M. Rutkowska, L. Chmielarz, M. Jabłońska, C.J. Van Oers, P. Cool, J. Porous Mater. 21 (2014) 91–98.
[38] G.S. Kumar, S. Saravanamurugan, M. Hartmann, M. Palanichamy, V. Murugesan, J. Mol. Catal. A: Chem. 272 (2007) 38–44.
[39] K. Sadowska, K. Góra-Marek, J. Datka, Vib. Spectrosc. 63 (2012) 418–425.
[40] K. Sadowska, K. Góra-Marek, M. Drozdek, P. Kuśtrowski, J. Datka, J. Martinez Triguero, F. Rey, Micropor. Mesopor. Mater. 168 (2013) 195–205.
[41] Q. Shen, L. Li, C. He, X. Zhang, Z. Hao, Z. Xu, Asia-Pac. J. Chem. Eng. 7 (2012) 502–509.
[42] Y. Li, D. Liu, W. Wang, S. Xie, X. Zhu, L. Xu, J. Nat. Gas Chem. 17 (2008) 69–74.
[43] P. Castaño, G. Elordi, M. Olazar, A.T. Aguayo, B. Pawelec, J. Bilbao, Appl. Catal. B: Environ. 104 (2011) 91–100.
[44] G. Elordi, M. Olazar, G. Lopez, P. Castaño, J. Bilbao, Appl. Catal. B: Environ. 102 (2011) 224–231.
[45] A.G. Gayubo, A. Alonso, B. Valle, A.T. Aguayo, J. Bilbao, Appl. Catal. B: Environ. 97 (2010) 299–306.
[46] A.G. Gayubo, A. Alonso, B. Valle, A.T. Aguayo, J. Bilbao, Ind. Eng. Chem. Res. 49 (2010) 10836–10844.
[47] Y. Sang, H. Liu, S. He, H. Li, Q. Jiao, Q. Wu, K. Sun, J. Energy Chem. 22 (2013) 769–777.
[48] A.A. Rownaghi, F. Rezaei, M. Stante, J. Hedlund, Appl. Catal. B: Environ. 119–120 (2012) 56–61.
[49] M. Stöcker, Micropor. Mesopor. Mater. 29 (1999) 3–48.
[50] G. Elordi, M. Olazar, G. Lopez, P. Castaño, J. Bilbao, Appl. Catal. B: Environ. 102 (2011) 224–231.